Contents lists available at ScienceDirect

Earth and Planetary Science Letters

journal homepage: www.elsevier.com/locate/epsl



The survival of tracers of primordial mantle heterogeneity investigated through ¹⁴²Nd/¹⁴⁴Nd and ³He/⁴He isotope decoupling in the Gorgona Island lavas



Eugenia Hyung ^{a,*}, Mauricio Ibañez-Mejia ^b, Yamirka Rojas-Agramonte ^c

- ^a Earth and Planetary Sciences, Harvard University, 20 Oxford St., Cambridge, MA 02138, USA
- ^b Department of Geosciences, University of Arizona, Tucson, AZ 85721, USA
- ^c Institut für Geowissenschaften, Christian-Albrechts-Universität zu Kiel, Ludewig-Meyn-Straße 10, 24118 Kiel, Germany

ARTICLE INFO

Article history: Received 26 May 2023 Received in revised form 30 August 2023 Accepted 15 September 2023 Available online xxxx Editor: R. Hickey-Vargas

Keywords: Gorgona Island Galapagos plume komatiites ³He/⁴He 142 Nd/144 Nd isotopes pyroxenite

ABSTRACT

While 142Nd/144Nd, 3He/4He, and 182W/184W isotope ratios are recognized and applied as tracers of primordial mantle heterogeneity, their distribution and reasons behind the extent of variability in the modern-day mantle remain unclear. Lavas associated with the Galapagos plume exhibit the steepest 3 He/ 4 He vs. μ^{182} W isotope correlations and thus hold the potential to elucidate the processes involved in the preservation of isotope variability. Among the various eruptions suggested to be related to the Galapagos plume is Gorgona Island, which is geologically significant for their Phanerozoic komatiites. We report the first high precision 142Nd/144Nd isotope measurements for the Gorgona komatiites, as well as ${}^{3}\text{He}/{}^{4}\text{He}$ and major and trace element data for an array of lavas including komatiites, a picrite, a dgabbro ("depleted"), and an e-basalt ("enriched"). The 142 Nd/144 Nd ratios of six komatiite samples are indistinguishable to within ± 2.4 ppm (2σ) from the modern-day terrestrial mantle as sampled by most mid-ocean ridge and ocean island basalts. The ³He/⁴He values determined for the komatiites and a picrite are from 4.6 to 45.1 R_A. Eight of the ${}^{3}\text{He}/{}^{4}\text{He}$ measurements are higher than the MORB average (8 \pm 1 $R_{
m A}$), and thus strongly point to a plume source sampling an undegassed reservoir. The $R_{
m A}$ value of 45.1 in particular ranks among the highest ³He/⁴He ratios measured to date at Gorgona Island and elsewhere, close to what is observed for Phanerozoic flood basalts from Baffin Island.

Evaluation of the sources of the lavas using major and rare earth elements along with $arepsilon^{143} \mathrm{Nd}$ signatures suggest that the komatiites and picrites are derived from a depleted peridotite source. Meanwhile, the e-basalts are deduced to have been derived from a hybrid source consisting of roughly 8% pyroxenite to 92% peridotite. The inferred and calculated degree of pyroxenite in the sources of the different lava types align with the magnitude of ${}^{3}\text{He}/{}^{4}\text{He}$ ratios observed. Model calculations involving pyroxenite sources in the e-basalts, which are reported to exhibit ¹⁸²W/¹⁸⁴W isotope anomalies, attest to their survival, while analogous calculations with 142 Nd/ 144 Nd isotope ratios suggest homogenization occurring on a faster timescale. It is deduced that 182 W/ 184 W anomalies are likely to outlast mixing with recycled pyroxenite compared to ¹⁴²Nd/¹⁴⁴Nd and ³He/⁴He ratios. The decoupling of modern-day ¹⁴²Nd/¹⁴⁴Nd, ³He/⁴He, and ¹⁸²W/¹⁸⁴W isotope variabilities thus likely reflect the sensitivity each system has to different mantle processes that contribute to their preservation throughout time.

© 2023 Elsevier B.V. All rights reserved.

1. Introduction

Driven by plate tectonics, the silicate Earth undergoes recycling through subduction and upwelling. Geochemical compositions of ocean island basalts (OIBs) that are distinct from those of mid-

* Corresponding author. E-mail address: hyung@fas.harvard.edu (E. Hyung).

ocean ridge basalts (MORBs) reflect the diverse geochemical com-

positions of the mantle. In particular, mantle plumes are thought to source geochemical signatures reflective of the deep mantle, evidenced by seismic tomographic models resolving conduits reaching below the 660-km discontinuity and well into the lower mantle (e.g., French and Romanowicz, 2015). OIBs are thought to sample the deep mantle, preserving primordial signatures that reflect early Earth differentiation and its evolution over time.

Tracers of early Earth differentiation include 142 Nd/144 Nd and ¹⁸²W/¹⁸⁴W ratios, expressed as deviations with respect to the modern-day bulk silicate Earth. Owing to the short half-lives of their parent isotopes ($^{182}{\rm Hf} \rightarrow ^{182}{\rm W}$, $t_{1/2}=8.9$ Myr; Vockenhuber et al., 2004; $^{146}{\rm Sm} \rightarrow ^{142}{\rm Nd}$, $t_{1/2}=103$ Myr; Marks et al., 2014; Meissner et al., 1987) the presence of anomalous signatures in $^{142}{\rm Nd}/^{144}{\rm Nd}$ and $^{182}{\rm W}/^{184}{\rm W}$ reflects chemical fractionation between the parent and daughter elements while the parent isotope was extant. On the other hand, $^3{\rm He}/^4{\rm He}$ ratios are considered a tracer of primordial heterogeneity as $^3{\rm He}$ can only be lost, while $^4{\rm He}$ is constantly generated through in-situ ingrowth due to the radioactive decay of Th and U. Therefore, low $^3{\rm He}/^4{\rm He}$ ratios are reflective of recycled materials or $^3{\rm He}$ loss by mantle degassing during partial melting through time.

Geochemical heterogeneity in OIBs is evidenced in modernday variability in 182W/184W isotopes in various OIBs associated with plume sources, which are often associated with high ³He/⁴He ratios to varving degrees (Mundl-Petermeier et al., 2020, 2019: Mundl et al., 2017). In contrast, there are few 142 Nd/144 Nd isotope anomalies that are considered to be resolved with respect to the present day mantle and are much less common compared to W isotope anomalies (Hyung and Jacobsen, 2020; Peters et al., 2021, 2018). Whereas ¹⁴²Nd/¹⁴⁴Nd and ¹⁸²W/¹⁸⁴W isotope anomalies that originate from silicate differentiation processes are expected to be coupled, reflecting the similar incompatible behavior of the parent nuclides during igneous processes, 142Nd/144Nd ratios have been observed to be decoupled from both high ³He/⁴He and ¹⁸²W/¹⁸⁴W ratios (Peters et al., 2021; Rizo et al., 2019), leading to the emergence of alternative hypotheses needed to explain the origins of W isotope anomalies. The core of the Earth has been proposed as one possible reservoir for the origin of modern-day ¹⁸²W/¹⁸⁴W isotope anomalies in the mantle (e.g., Ferrick and Korenaga, 2023; Mundl-Petermeier et al., 2020; Rizo et al., 2019). This is due to its inferred low ¹⁸²W/¹⁸⁴W isotope ratio relative to the bulk silicate Earth owing to the siderophile nature of tungsten during core-mantle differentiation (e.g., Kleine et al., 2002), supported by W isotope studies of iron meteorites (e.g., Kruijer et al., 2014).

Basalts associated with the Galapagos plume exhibit the steepest ³He/⁴He correlations with ¹⁸²W/¹⁸⁴W ratios yet observed (Mundl-Petermeier et al., 2020). Meanwhile, the e-basalts ("enriched") at Gorgona Island, present an enigma due to their ¹⁸²W/¹⁸⁴W anomalies but high ¹⁸⁷Os signatures (Walker et al., 2021). Gorgona Island is characterized by its diverse rock compositions and holds petrologic significance as it hosts the only known spinifex-textured ultramafic lavas (komatiites) to occur in the Phanerozoic (Aitken and Echeverría, 1984). Although its connections are debated (e.g., Serrano et al., 2011; Boschman et al., 2014), Gorgona Island has been widely associated with the Galapagos plume (Duncan and Hargraves, 1984; Kerr, 2005; Soderman et al., 2023; Storey et al., 1991; Trela et al., 2017). Gorgona Island thus provides a key setting for understanding the origin and recycling of short-lived radiogenic isotope tracers and potential in association with primitive ³He/⁴He ratios from deep-seated plumes. Investigating the petrogenic relationships and origins of these lavas that sample the deeper parts of the mantle is expected to elucidate the survival of these primordial tracers and enhance the interpretation of these signatures by providing further insights into the processes responsible for their long-term preservation, or lack of thereof.

We present major element, trace element, and high-precision 142 Nd/ 144 Nd isotope ratios and 3 He/ 4 He data from a set of samples from Gorgona Island, which include six komatiites, one e-basalt, one d-gabbro ("depleted"), and a picrite. Major and trace element data are used to infer and quantify the presence and amount of pyroxenite in the sources of the various lavas. These constraints are further used to hypothesize and understand the factors that contributed to the survival and homogenization of 142 Nd/ 144 Nd,

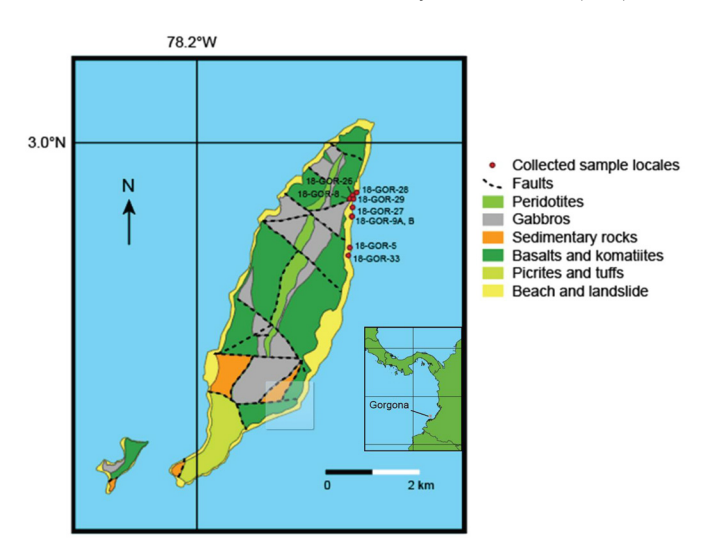


Fig. 1. Sampling locations of the komatiites, e-basalt, d-basalt, and picrite for this study. The geology of Gorgona Island is based on Echeverría (1980).

 $^{3}\mathrm{He}/^{4}\mathrm{He}$, and $^{182}\mathrm{W}/^{184}\mathrm{W}$ isotope ratios in the terrestrial mantle throughout time.

2. Geology and tectonics

Gorgona is a small island located off the Colombian coast and is a host to a wide range of rock types including e-("enriched") and d-basalts ("depleted"), gabbros, dunites, wehrlites, picrites, and Phanerozoic komatiites (Fig. 1), for which it holds geologic significance (Aitken and Echeverría, 1984; Kerr et al., 1996; Kerr, 2005; Révillon et al., 2000a). The geology of the island has been studied and described in detail in Aitken and Echeverría (1984) and Kerr et al. (1996). Volcanic rocks are mainly accessible along the coast due to the thick rain forests in the inner part of the island (Dietrich et al., 1981; Révillon et al., 2000a). The lavas on Gorgona Island are associated with the Caribbean Plateau, which in turn has been commonly accepted to have connections to the Galapagos plume (e.g., Duncan and Hargraves, 1984; Storey et al., 1991; Trela et al., 2015, 2017; Soderman et al., 2023). However, the degree of influence of the Galapagos plume on the lavas of Gorgona Island remains a controversial topic (e.g., Boschman et al., 2014; Kerr and Tarney, 2005; Serrano et al., 2011). The samples for this study were collected along the northeast shore of Gorgona Island from Playa Bonita, Playa Yundigua, Quebrada Playa, and Playa Pizarro (Fig. 1).

3. Methods

3.1. Sample preparation and measurements

Specimens were carefully cut with a Gorilla blade diamond saw to remove alteration from weathering. The pieces were then polished with SiC sandpapers of 80–100 grit sizes on a polishing wheel to remove any traces of sawing. The 1–2 inch pieces were sonicated in ethanol and deionized water and subsequently crushed in a hydraulic press between multiple layers of paper and plastic zip-lock bags to avoid contamination from metal. The 0.5 cm-size pieces retrieved from this process were ground in an alumina mortar in a shatterbox for major, trace element, and isotopic analysis. Rock fragments not subjected to the grinding process were set aside for noble gas analysis. All sample preparation involving dissolution and column chromatography was performed in the Isotoparium clean lab at California Institute of Technology using the methods of Hyung and Tissot (2021).

Sample powders were analyzed for their loss on ignition data by heating them at 100 °C for over six hours and then in a furnace at 1500 °C for one hour. Samples were analyzed for their major elements using an INAM Expert 3L tabletop XRF with a Ti target using its built-in fundamental parameter software. For trace element analysis, a small aliquot (5 mg equivalent) was diluted in 3% HNO₃ spiked with 10 ppb In as an internal standard (Al-Hakkani, 2019). Calibration standards were prepared by diluting Spex CLMS multi-element solutions to 1, 4, and 10 ppb. To correct for any systematic offsets in concentration measurements, BHVO-2 was measured as an unknown and used to correct the data (Jochum et al., 2005). Samples were typically diluted by a factor of ~5000. Measurements were made in STD mode and KED mode using He as a collision cell gas on the iCAP RQ (ThermoScientific) at the Caltech Isotoparium.

Helium isotope measurements (3 He/ 4 He) were obtained from whole rock samples via in-vacuum crushing using a Thermo Scientific Helix SFT noble gas mass spectrometer using established analytical procedures at the Caltech Noble Gas lab (e.g., Balbas and Farley, 2020). Blanks were typically within 5% of the measured helium. The 1σ uncertainties were within ± 0.4 R_A (R_A = 3 He/ 4 He_{atmosphere}) with the exceptions of samples 18-GOR-8 and 18-GOR-29 and the mineral separates of 18-GOR-29, which exhibited higher uncertainties between 1.9–2.2 R_A. The 1σ uncertainties of the fusion measurements were between 0.10–0.22 R_A and determined to be inconsequential.

Sample matrices were subjected to fusion analysis to check for cosmogenic He. Mineral separates of 18-GOR-29 were acquired to measure their ³He/⁴He ratios, by sorting grains between sizes of 0.5–1 mm through sieves of 100-200 mesh size. Magnetite was further picked out with a hand-magnet before processing the samples through a Frantz at 0.2 A and 0.4 A. A rough collection of the darker, more magnetized grains consisting of a mixture of olivine, clinopyroxene, and spinel were measured for their ³He/⁴He ratios.

Fractions between 100–600 mg of powder were digested and processed for each komatiite sample. Neodymium fractions were chemically purified using the methods of Hyung and Tissot (2021). In summary, the rock powders obtained from sample preparation were dissolved in a mixture of HF-HNO $_3$ at 180 °C overnight and then subsequently dried down. The remaining residuals were then redissolved in aqua regia at 180 °C and dried down. The solution was dissolved in 1.5 N HCl and processed through cation exchange columns to separate the REEs from the matrix. The resulting REE cut was dried down, treated with H_2O_2 for oxidation and removal of Ce, and then processed twice through pressurized α -HIBA cation exchange columns for a purified Nd cut. Neodymium blanks were typically around 50 pg.

Neodymium isotopes were acquired with a ThermoFisher Scientific Triton TIMS at the Isotoparium lab at Caltech following the techniques of Hyung and Tissot (2021). About 1 µg of Nd was loaded onto a filament for each measurement. $^{142}\rm{Nd}/^{144}\rm{Nd}$ isotope measurements consisted of two-line multi-dynamic acquisitions with an integration time of 8.389 secs, a magnet idle time of 3 secs, and a baseline measurement every five blocks consisting of ten cycles each. Raw runs were corrected for isobaric interferences and mass fractionation using the exponential law and a normalization ratio of $^{146}\rm{Nd}/^{144}\rm{Nd} = 0.7219$. The data were reduced according to the principles of Reduction Method 2 outlined in Hyung and Jacobsen (2020).

3.2. Nonmodal batch melting calculations

REE modeling of the e-basalts and gabbros from Gorgona Island was carried out assuming a spinel lherzholite composition for the peridotite component. REE concentrations for the pyroxenite component were derived by partially melting DMM to varying degrees and compared with results from N-MORBs. Calculations were performed considering two different types of peridotite compositions,

namely, the depleted MORB mantle (DMM) of Workman and Hart (2005) and the bulk silicate Earth (BSE) of McDonough and Sun (1995).

Incremental nonmodal batch melting calculations were performed using modes from Workman and Hart (2005) and from typical garnet peridotites used in experiments (Walter, 1998). Melt reactions are taken from Baker and Stolper (1994), Kinzler and Grove (1992), and Pertermann and Hirschmann (2003), and Walter (1998). Partial melts of pyroxenite-peridotite mixtures are derived by mixing separately melted pyroxenite and peridotite compositions following the study of Sobolev et al. (2007). Full modeling parameters are compiled in the Supplementary Material.

4. Results

4.1. Major element data and classification

The MgO contents of the samples ranged from 7.4 to 31.37 wt%. Six samples were observed to display spinifex textures. The combined ranges of the MgO, Na₂O+K₂O and TiO₂ contents of three of these six samples (18-GOR-8, 18-GOR-9A, B) place the samples in the range of picrites following the IUGS classification scheme of Le Bas (2000) on a volatile-free basis. One sample (18-GOR-27) is classified as a basanite. Six samples (18-GOR-8, 18-GOR-9A, 18-GOR-9B, 18-GOR-27, 18-GOR-28, 18-GOR-33; Table 1) are referred to as komatiites for this study hereinafter following the recommendations of Kerr and Arndt (2001) and Kerr (2005) on the basis of their spinifex textures. Only two samples (18-GOR-28, 18-GOR-33) are strictly considered to be komatiites following the IUGS classification scheme. While the high MgO sample (18-GOR-29) may similarly be classified as a komatiite according to the IUGS classification scheme, it was observed to lack a spinifex texture and is referred to as a picrite in this study to be able to similarly compare with other Gorgona lavas referred to as picrites throughout the literature. The extent of alteration and volatile content of the samples were reflected on the loss on ignition, which varied between 3.6-4.5 wt%. Major element and loss on ignition data are reported in Table S1 in the Supplementary Material.

4.2. Trace element data

Five komatiites in this study were determined to be G2 komatiites on the basis of their Zr and La concentrations as well as their $(Gd/Yb)_N$ ratios following the work of Révillon et al. (2000a) (Fig. 2). Sample 18-GOR-26, a basalt, is identified to be an e-basalt based on its mildly enriched LREE pattern similar to the e-basalts in the literature. A sample of a microgabbro, 18-GOR-5, is identified to be a d-gabbro based on its major element composition and degree of LREE depletion. Sample 18-GOR-29 is markedly depleted in its LREE pattern in comparison to other komatiites in this study (Fig. 3d). The e-basalt was the only sample in this study that was noted to be mildly enriched in LREE. Based on their $(Gd/Yb)_N$ and Ce/Sm ratios (Fig. 2), five of the six komatiites in this study are inferred to be G2 komatiites.

4.3. Noble gas data

Measurements of ${}^{3}\text{He}/{}^{4}\text{He}$ varied between 4.6–39.5 R_A for whole rock sample crushes (Table 1, Fig. 4). Among the various sample types, the picrite sample (18-GOR-29) was exhibited to have the highest R_A value among the samples measured in this study. The separated mineral fraction from the picrite sample had a measured R_A of 45.1. The R_A values of five komatiites were similar to those of OlBs, varying between 11.9–31.4, with one komatiite sample (18-GOR-8) displaying an R_A of 4.6. The e-basalt (18-GOR-26) exhibited an R_A of 6.9. The microgabbro (18-GOR-5)

Table 1 Helium and Nd isotope measurements of Gorgona Island lavas.

Sample Name	³ He/ ⁴ He (R _A) ^a	1σ	He whole rock mass (g)	Fusion	1σ	⁴ He ncc STP/g	He blank (fraction)	$\mu^{142} \mathrm{Nd^b}$	2σ	¹⁴⁷ Sm/ ¹⁴⁴ Nd	$\varepsilon^{143} \mathrm{Nd_{(T)}}^{c}$	2σ
18-GOR-8	4.6	2.2	1.061	3.0	0.18	6.02	0.00524	-1.9	3.3	0.3328	9.20	0.029
18-GOR-8 replicate(Nd)e								-2.9	2.3		9.08	0.027
18-GOR-9A	31.4	0.67	1.054	4.1	0.15	4.48	0.00561	-2.3	2.4	0.3367	9.06	0.027
18-GOR-9B	23.0	0.47	1.055	4.5	0.21	3.47	0.0194	-0.1	4.1	0.3517	9.04	0.037
18-GOR-9B replicate								0.7	3.6		9.02	0.026
18-GOR-27	11.9	0.21	0.901	7.7	0.22	2.23	0.00129	0.9	3.0	0.3348	7.01	0.032
18-GOR-27 replicate								0.4	2.7		7.01	0.030
18-GOR-28	14.1	0.42	1.328	6.2	0.18	9.49	0.0244	0.7	2.3	0.3461	8.91	0.025
18-GOR-28 replicate								1.6	3.0		8.85	0.033
18-GOR-33	13.0	0.44	0.786	2.3	0.10	2.05	0.0109	1.1	2.1	0.2911	10.10	0.024
18-GOR-5	10.7	0.22	1.213	3.0	0.10	10.67	0.00141					
18-GOR-26	6.9	0.36	2.720	0.2	0.20	0.46	0.555					
18-GOR-29	39.5	1.3	1.085	5.3	0.13	1.33	0.0188					
18-GOR-29 mineral separates ^d	45.1	1.9	0.435	6.5	0.17	2.25	0.0122					

Whole rock sample crushes.

^e Mineral separates.

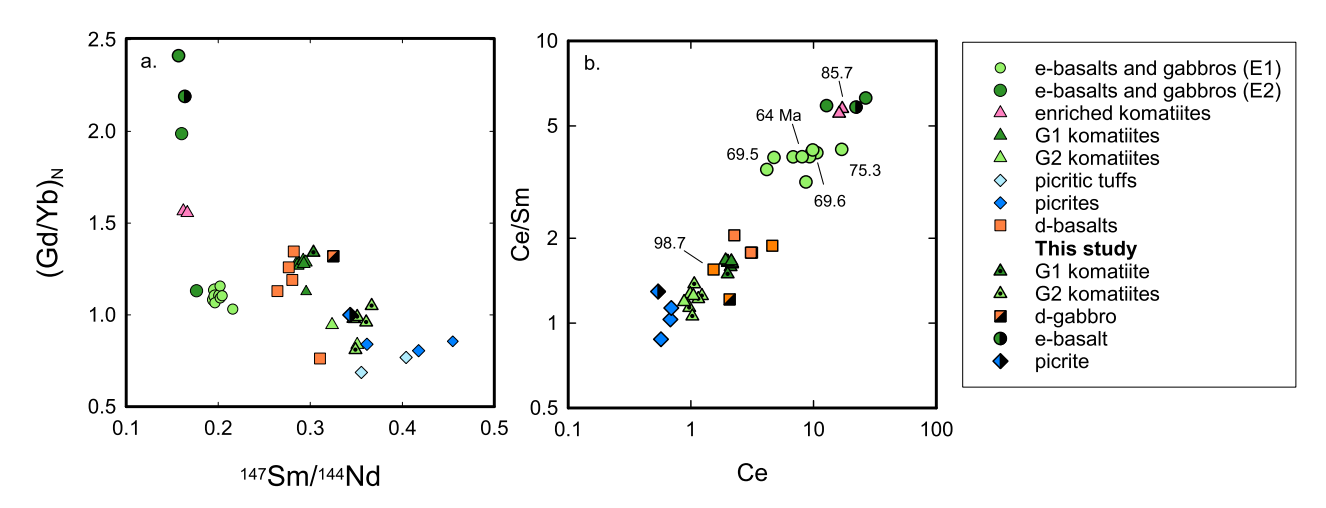


Fig. 2. Normalized Gd/Yb vs 147 Sm/144 Nd ratios (a) and Ce/Sm vs Ce concentrations (b) of the samples of this study plotted with respect to dated samples. The Ce/Sm vs Ce concentrations of the microgabbro of this study plots near other d-basalts (orange squares) and G1 komatiites. The Ce/Sm ratios of the komatiites from this study (triangles with dots) may be grouped with the G2 komatiites (light green triangles) except for one sample which plots closer to the G1 komatiites. Picrites and picritic tuffs are represented with diamonds, while e-basalts are represented with green circles. The ages of samples are indicated in Ma.

was measured to have an RA of 10.7. Fusion experiments yielded R_As between 2.3–7.7, lower than the ³He/⁴He ratios of whole rock crushes, suggesting that cosmogenic helium is not a significant contributor to the high ³He/⁴He ratios of the samples in this study.

4.4. Nd isotope data

Six komatiite samples were measured for their $^{142}\mathrm{Nd}/^{144}\mathrm{Nd}$ and ¹⁴³Nd/¹⁴⁴Nd ratios, with four samples subjected to repeat dissolutions and measurements. The 142Nd/144Nd ratios of JNdi-1 were generated at an external precision of ± 2.4 ppm (2σ) from a combination of JNdi-1 and reference materials (n = 15; published in Hyung and Tissot, 2021), and were determined over a similar time period of the results reported here. The ¹⁴²Nd/¹⁴⁴Nd values of the six komatiite samples studied demonstrate no resolvable variability with respect to the average modern-day mantle (Fig. 4). Interferences for ¹⁴²Ce/¹⁴²Nd were unusually high and ranged from 1 to 10 ppm, and ¹⁴⁴Sm/¹⁴⁴Nd varied between sub-ppm, with one sample at 9 ppm. Despite higher-than-normal interference levels, the ten ¹⁴²Nd/¹⁴⁴Nd isotope measurements of the samples were observed to agree closely, and all plot within $2\sigma = \pm 2.4$ ppm (Fig. 4) with a 2σ standard deviation of ± 3.2 ppm. Age-corrected $\varepsilon^{143} Nd$ values of the komatiites ranged between 7.0-10.1 assuming an eruption age of 89 Ma. Such 142Nd/144Nd values are expressed in terms of deviations from INdi-1 in parts per million (μ^{142} Nd), while ¹⁴³Nd/¹⁴⁴Nd values are deviations from INdi-1 expressed in parts per 10,000 (ε^{143} Nd) throughout this study and are summarized in Table 1. The ¹⁴⁷Sm/¹⁴⁴Nd ratios have been calculated from trace element concentrations.

5. Discussion

5.1. Subclassification and groupings of the various Gorgona lavas

E-basalts largely demonstrate two types of REE patterns, one whose bulk silicate Earth (BSE) normalized REE patterns are flat for both LREE and HREE, and another that is mildly enriched in LREE. REEs individually plotted with respect to Th concentrations in log-log space also demonstrate two major groups within the ebasalts, each corresponding to the types of REE patterns exhibited for each group (Fig. 5). Linear trends in log-log space likely reflect the extent of differentiation through fractional crystallization

whole lock sample citaties.

b Relative to JNdi-1. μ^{142} Nd = $(^{142}$ Nd/ 144 Nd_{sample} - 142 Nd/ 144 Nd_{std}) $)^{142}$ Nd/ 144 Nd_{std} x 10⁶.

c Age-corrected to 89 Ma. ϵ^{142} Nd = $(^{142}$ Nd/ 144 Nd_{sample} - 142 Nd/ 144 Nd_{cHUR})/ 142 Nd/ 144 Nd_{cHUR} x 10⁴ where 143 Nd/ 144 Nd_{cHUR} = 0.512638.

d Replicate measurements refer to Nd isotope measurements.

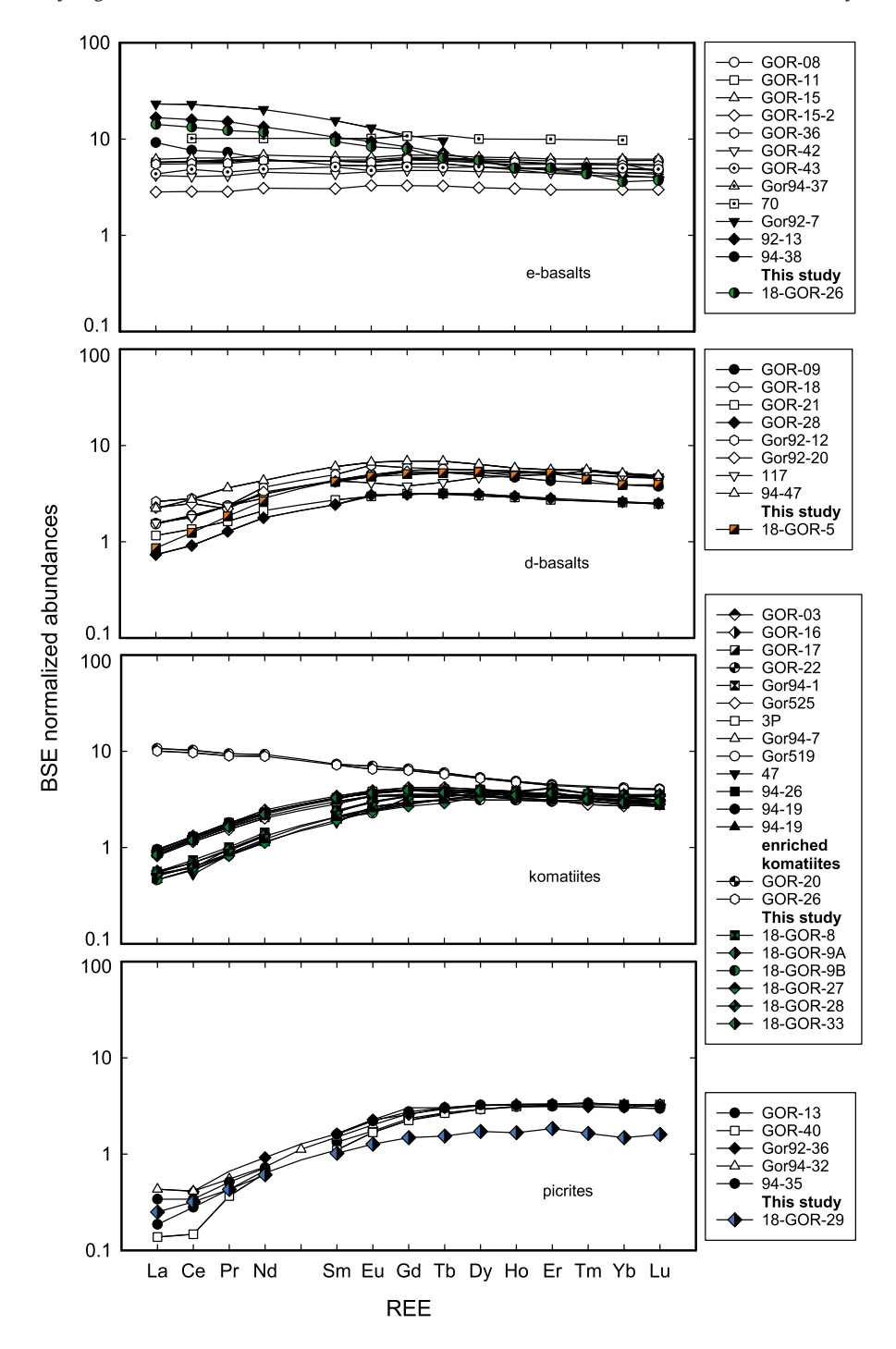


Fig. 3. REE patterns of (a) e-basalts, (b) d-basalts, (c) komatiites, and (d) picrites from different literature sources (Aitken and Echeverría, 1984; Arndt et al., 1997; Brügmann et al., 1987; Dupré and Echeverría, 1984; Echeverría, 1980; Echeverría and Aitken, 1986; Kerr, 2005; Révillon et al., 2002, 2000a; Serrano et al., 2011; Walker et al., 1999) and this study (colored symbols).

from separate parental magmas for each group. These observations enable us to categorize the e-basalts into two groups: the "E1" basalts, which are associated with flat REE patterns, and the "E2" basalts, which exhibit mildly enriched LREE patterns. The REE vs Th concentrations of the two enriched komatiites from the study of Serrano et al. (2011) are observed to plot closely to the E2 basalts, suggesting close petrogenetic ties.

Komatiites and picrites from Gorgona Island have been extensively modeled and studied (Echeverría and Aitken, 1986; Kerr et al., 1996; Kerr, 2005; Révillon et al., 2000a) and are deduced to have been generated through dynamic melting (a fractional melt-

ing process where a small fraction of the melt remains in the residue) of a depleted mantle source (Arndt et al., 1997; Révillon et al., 2000a). The komatiites have been divided into two groups, G1 and G2, based on compositional differences such as TiO_2 content, their trace element ratios, and HREE patterns (Révillon et al., 2000a). The flat HREE patterns of the G2 komatiites have been interpreted to indicate that melting started in the garnet stability field and continued in the spinel stability field (Révillon et al., 2000a), while G1 komatiites have been characterized to have melted in the garnet stability field.

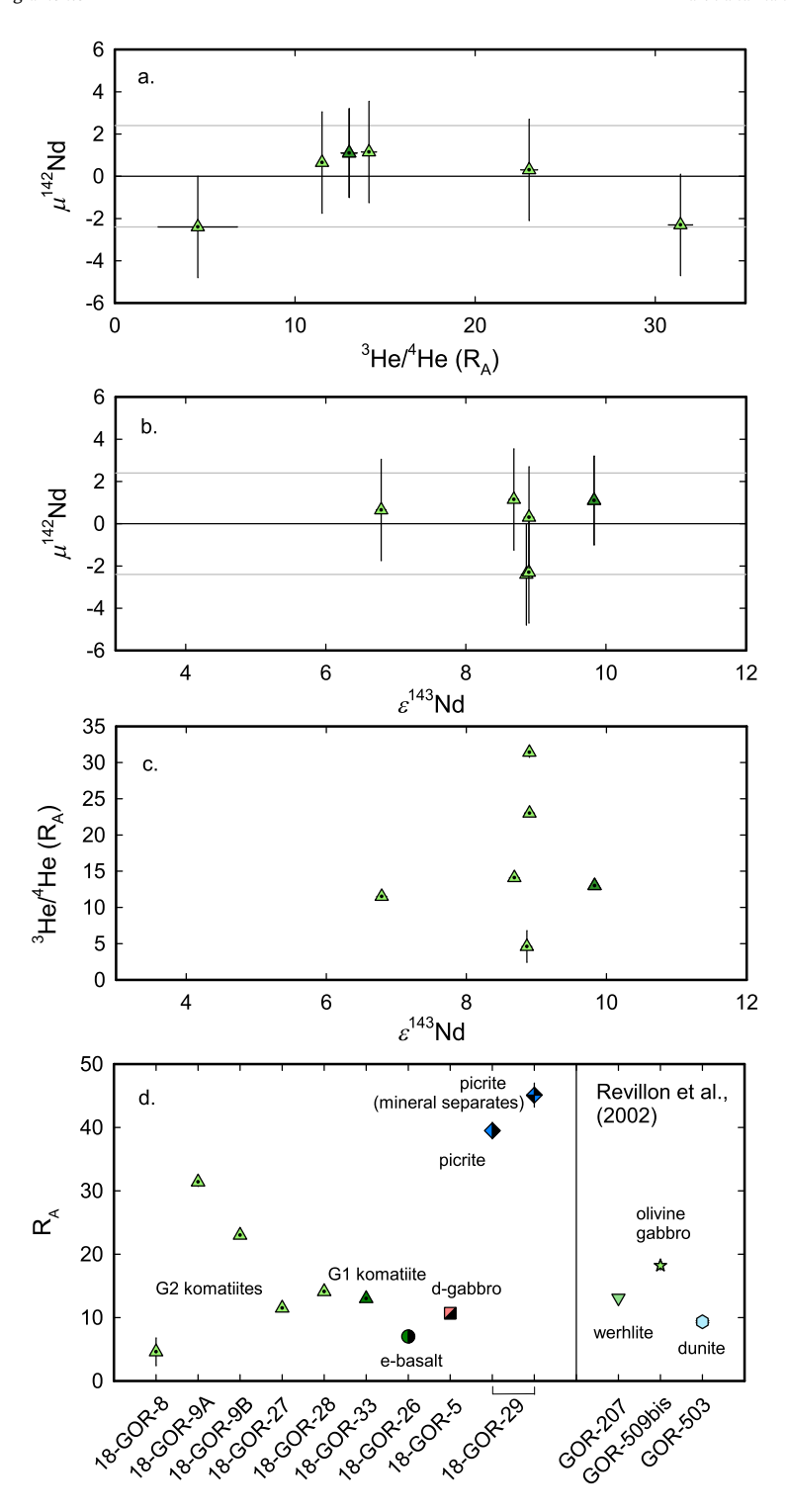


Fig. 4. Plots of sample μ^{142} Nd, ε^{143} Nd, and 3 He/ 4 He measurements in R_A. The plots demonstrate lack of 142 Nd/ 144 Nd isotope variability across a range of 3 He/ 4 He and ε^{143} Nd values. High R_A are associated with depleted 143 Nd/ 144 Nd ratios. Error bars are presented in 2σ for μ^{142} Nd, and 1σ for 3 He/ 4 He. The horizontal lines in (a) and (b) represent 2σ external precision error from the JNdi-1 standard and reference materials (n = 15; 2σ = ±2.4 ppm). Repeat sample μ^{142} Nd measurements are averaged and plotted with 2σ external precision error bars. Plotted for comparison in panel (d) on the right-hand side are the highest reported R_A values for olivine separates of different Gorgona samples studied in Révillon et al. (2002).

E1 basalts demonstrate a range of age-corrected ε^{143} Nd values varying from 7.02 to 7.82 (T=64–75.3 Ma), with one sample at 5.5 (T=89 Ma). The ε^{143} Nd values of E2 basalts (Arndt et al., 1997) are generally lower than those of E1 basalts, varying from 5.4–7.0. One sample categorized as an enriched komatiite, has been measured to have an ε^{143} Nd value of 5.6 (Serrano et al., 2011), within the range of the E2-basalts.

5.2. The heterogeneous sources of the Gorgona lavas inferred from major element compositions

Different studies (Arndt et al., 1997; Echeverría and Aitken, 1986; Kerr et al., 1996; Kerr, 2005) have noted that the range of trace and isotopic element compositions present in the Gorgona lavas, which include the picrites, komatiites, and basalts likely re-

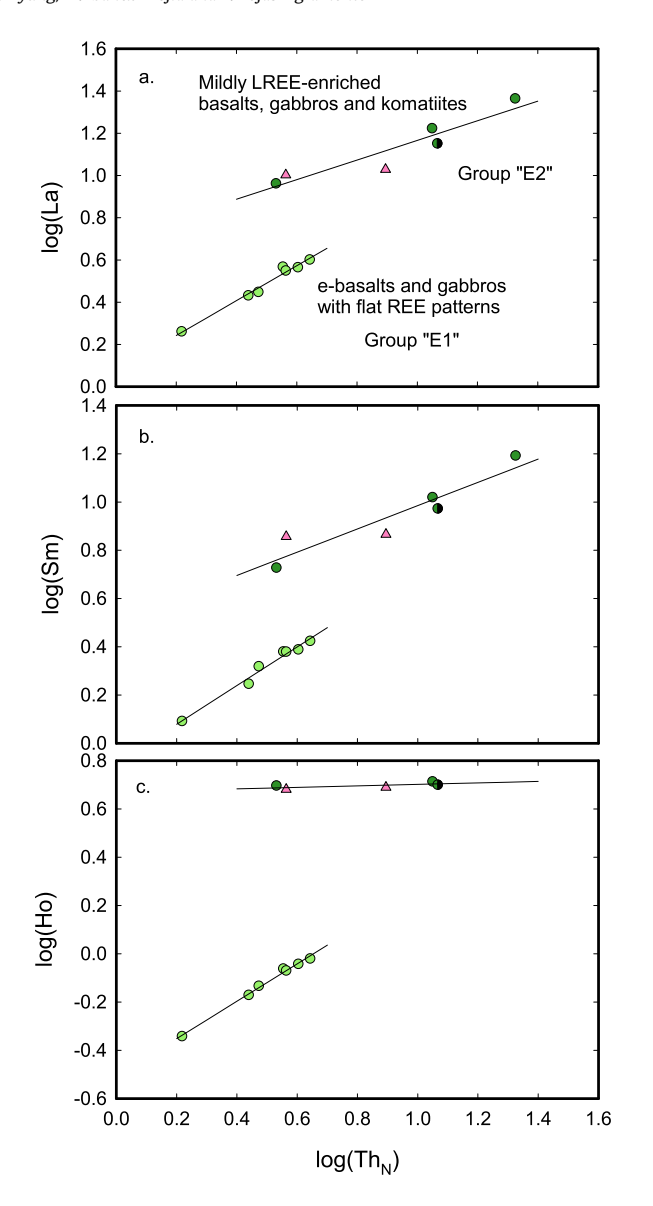


Fig. 5. Concentrations of (a) La, (b) Sm, and (c) Ho of e-basalts and enriched komatites plotted with respect to Th concentrations in log-log space. The pink triangles represent the enriched komatiites, the circles, the e-basalts, and the half-filled circle represents the e-basalt from this study. The data largely cluster into two groups, where linear correlations to a first order are interpreted to represent fractional crystallization trends from two separate parental magmas.

flect a number of distinct mantle sources. In this study, we use comparisons with major element compositions from experimental melts and proxies for pyroxenite sources to understand the sources of the different rock types. The aim is to understand the components that affect the He, Nd, and W isotopic compositions that characterize the lavas and draw broader inferences with respect to their homogenization and preservation.

Melts from pyroxenite sources are recognized for their low CaO content due to the compatibility of Ca in clinopyroxene, which is abundant in pyroxenite. This observation has led to the identification of basalts from pyroxenite sources through their high FeO/CaO values at a given MgO/SiO₂ weight percent ratio. Numerical values higher than 0.65 at a given FeO/CaO – 3MgO/SiO₂ ("FC3MS factor") value have been proposed to represent lavas from a pyroxenite source (Yang and Zhou, 2013). The consumption of olivine during partial melting when pyroxenite is involved leads to higher FC3MS values as the MgO content in the melt decreases. An experimental melt generated from a source that is composed of equal

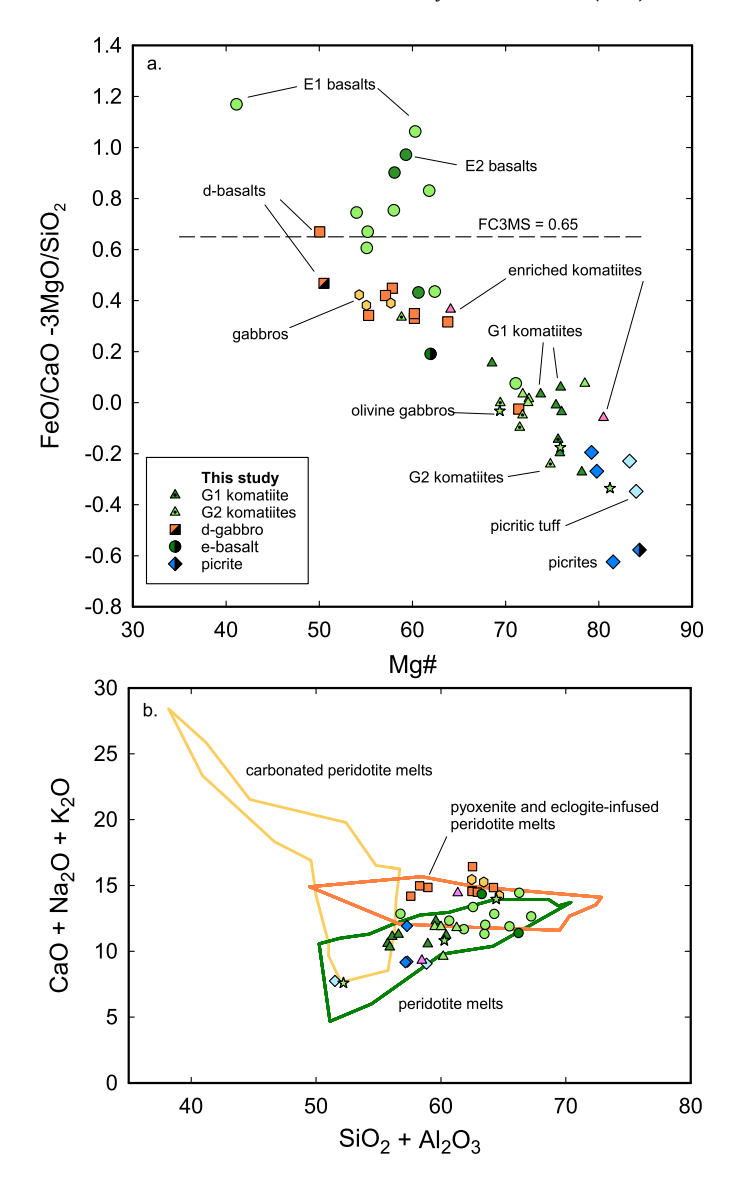


Fig. 6. (a) The FC3MS values (FeO/CaO - 3MgO/SiO $_2$ in wt%) of the Gorgona lavas from this study and throughout the literature, plotted with respect to their Mgnumber, calculated through Mg/(Fetot+Mg) \times 100 in molar proportions. (b) Outlines of CaO+Na $_2$ O+K $_2$ O vs SiO $_2$ +Al $_2$ O $_3$ contents of experimental melts plotted with data from picrites, tuffs, e- and d-basalts, and komatilites. The full range of experimental melts are plotted in Hyung et al. (2023).

parts pyroxenite and peridotite may lack olivine entirely (Mallik and Dasgupta, 2012). High (>0.65) FC3MS values are observed for experimental melts derived from one part basalt and two parts peridotite (Kogiso et al., 1998). Melting calculations also suggest that a small percentage (5–12%) of pyroxenite in a source may be sufficient to generate a pyroxenite-dominant melt (Shorttle and Maclennan, 2011). Although the FC3MS factor is a useful indicator for assessing the presence of pyroxenite in the source, there are limitations to the extent of inferences that can be made, and thus the FC3MS factor here is only used to confirm the presence of pyroxenite in lava sources, rather than constrain its abundance as it does not directly indicate the degree of pyroxenite present.

Plotted in Fig. 6a are the FC3MS vs Mg-number values of the Gorgona samples from this study as well as from the literature to determine whether there are lavas from Gorgona that originate from a pyroxenite source. It is observed that a majority of e-basalts generally plot in the domain (FC3MS > 0.65) strongly indicating the presence of pyroxenite in their sources. D-basalts have lower FC3MS values than those of the e-basalts, but higher val-

ues than those of komatiites and picrites, with at least one sample exceeding the 0.65 threshold value. This suggests the presence of pyroxenite in their source as well, but to a lesser extent than that of e-basalts.

Further comparisons are made between the major element compositions of experimental melts and the Gorgona lavas to discern their source materials. Gorgona samples from the literature and experimental melts with different starting compositions are plotted with respect to their CaO+Na₂O+K₂O vs SiO₂+Al₂O₃ contents for comparison (Fig. 6b). Different regions consisting of experimental melts from different starting compositions have been outlined in our diagram. Most of the samples that have been classified as d-basalts are found to overlap entirely with the regions composed of experimental melts from pyroxenites and eclogite-infused peridotite melts. This comparison further supports the presence of pyroxenite in the source of the d-basalts, although the FC3MS values indicate this is to a lesser degree than the sources of the e-basalts.

In contrast, komatiites and picrites generally plot in the domain comprising experimental melts derived from volatile-free peridotites. The CaO+Al₂O₃ vs SiO₂+Na₂O+K₂O compositions of the komatiites and picrites indicate that their sources are most similar to peridotite compositions. This observation is consistent with a depleted peridotite mantle origin for the komatiites and picrites (Arndt et al., 1997; Révillon et al., 2000a), which are thought to originate from the hottest and deepest parts of a plume (Kerr et al., 1996; Kerr, 2005; Révillon et al., 2000a).

To summarize, the e-basalts, and to a lesser extent, the d-basalts, are likely to have pyroxenite in their source lithology. Comparison of major element compositions of komatiites and picrites to those of experimental melts are consistent with a depleted peridotite mantle origin. The d-basalts, e-basalts, and depleted komatiites do not share the same petrogenetic origin (Arndt et al., 1997; Kerr et al., 1996; Kerr, 2005), and it is deduced that the degree of pyroxenite in the lava sources is an important component that contributes to the diverse compositional range of Gorgona lavas.

5.3. Characterizing the peridotite component of the source of the Gorgona lavas

Five komatiite samples analyzed in this study display depleted $arepsilon^{143} \mathrm{Nd}$ signatures (8.8–9.8), consistent with an origin from a mantle source that is highly depleted. However, one komatiite (18-GOR-27) is characterized to have a slightly more enriched ε^{143} Nd signature (7.0) than those of other komatiites in this study and elsewhere (Arndt et al., 1997; Serrano et al., 2011). Lower ε^{143} Nd values similarly observed in various Gorgona rocks, such as for the e-basalts (ε^{143} Nd = 5.5–7.8), a dunite (ε^{143} Nd = 5.3; Révillon et al., 2000a), olivine gabbros with depleted LREE patterns similar to picrites (ε^{143} Nd = 6.6-7.6; Révillon et al., 2000a), and a picrite with a flat LREE pattern (GOR92-37; Kerr, 2005) suggest the involvement of a slightly more enriched component in the peridotite source in addition to a depleted mantle reservoir. The moderately depleted $\varepsilon^{143} Nd$ signatures of the samples ($\varepsilon^{143} Nd =$ 5.5-7.8) compared to those that are highly depleted (>8.5), characterize this second reservoir to be distinct from the strongly depleted mantle source of the Gorgona komatiites and picrites. The LREE patterns, which are observed to be depleted in the majority of the aforementioned samples, imply that the secondary source is unlikely to be highly enriched in trace elements. Therefore, this reservoir is provisionally characterized to be analogous to the BSE in trace elements and ε^{143} Nd.

5.4. Constraining the amount of pyroxenite in the source of the *e-hasalts*

The petrogenesis of the Gorgona e-basalts, considering the presence of pyroxenite in their source, is underexplored. In this section, the melting processes and type of source involved in generating the parental magmas of the Gorgona e-basalts are explored by modeling the REE patterns of the different rock types simultaneously with the ε^{143} Nd isotope compositions of the lavas. In addition, as the degree of pyroxenite source contribution through major element analysis (Section 5.2.) suggest that a more than a minor (>1%) amount is necessary, this consideration is reflected in calculations. E-basalts generally exhibit a slight enrichment in LREE or flat patterns when normalized with respect to the BSE (Fig. 3a). The inferred degree of pyroxenite melt contribution will be used to explore their role in the survival of 182 W/ 184 W and 142 Nd/ 144 Nd isotope anomalies in the next section.

The REE patterns of the e-basalts exhibit two trends, flat vs mildly enriched patterns, corresponding to two groups of ε^{143} Nd isotope signatures. This indicates that the e-basalts were derived from two different parental magmas as discussed in section 5.2. To account for the two groups, E2-basalts have been modeled separately from the E1-basalts. Here ε^{143} Nd isotopes are used as an additional constraint to narrow the range of possible scenarios. First, it is deduced that primary magmas would generally exhibit lower LREE concentrations compared to more differentiated lavas as REEs are incompatible in most upper mantle minerals. Thus, the least concentrated REE patterns of the Gorgona e-basalts throughout the literature are interpreted to be least differentiated and this composition is set as an upper limit for the primary magmas.

An explanation proposed for flat LREE patterns relative to the BSE from the Caribbean Plateau involve pooled melts generated at depths through fractional melting that is homogenized during ascent (Révillon et al., 2000b). The calculations and considerations for the inferred source compositions for Gorgona e-basalts have typically involved a depleted peridotite source (Arndt et al., 1997; Révillon et al., 2000b). In lieu of the significant presence of pyroxenite inferred for the e-basalts in this study however, we model REE patterns with pyroxenite in the source.

LREE enrichment patterns of the E2-basalts are generally indicative of garnet in the source, whereas flat HREE patterns suggest the presence of spinel. Here the garnet signature is attributed to an eclogitized MORB-like pyroxenite component. For simplicity, a spinel peridotite source is assumed for partial melting calculations involving the depleted peridotite component and revisited. Two different types of peridotite sources are invoked (BSE and DMM) and their proportions are adjusted prior to partial melting, using $\varepsilon^{143} \mathrm{Nd}$ isotopes as a constraint in the degree of each type of source present. The BSE and DMM end-members are invoked as isotopically well-defined components for the purpose of further disentangling the degree of involvement of possible reservoirs that harbor primordial isotope signatures.

Model parameters that satisfy the constraints of REE enrichments, ε^{143} Nd isotopes, and the proportion of pyroxenite in the source exceeding 5% are summarized in Table S7 while resulting calculations are presented in Fig. 7b, c. The primary magma of the E2-basalts is modeled from nonmodal batch melting of the DMM, mixed with a BSE-like peridotite source at a proportion of 8%. The pyroxenite component is considered to have melted to F=0.20–0.25 and mixed with the spinel peridotite component melted to F=0.15–0.20 to produce a range of primary magmas. The flat REE patterns of the E1-basalts may similarly be modeled with an eclogite generated from a pyroxenite component calculated by nonmodal batch melting the DMM to F=0.07 and mixed with the hybrid peridotite source at a proportion of 8%. In contrast, calculations with N-MORB were difficult to match with the

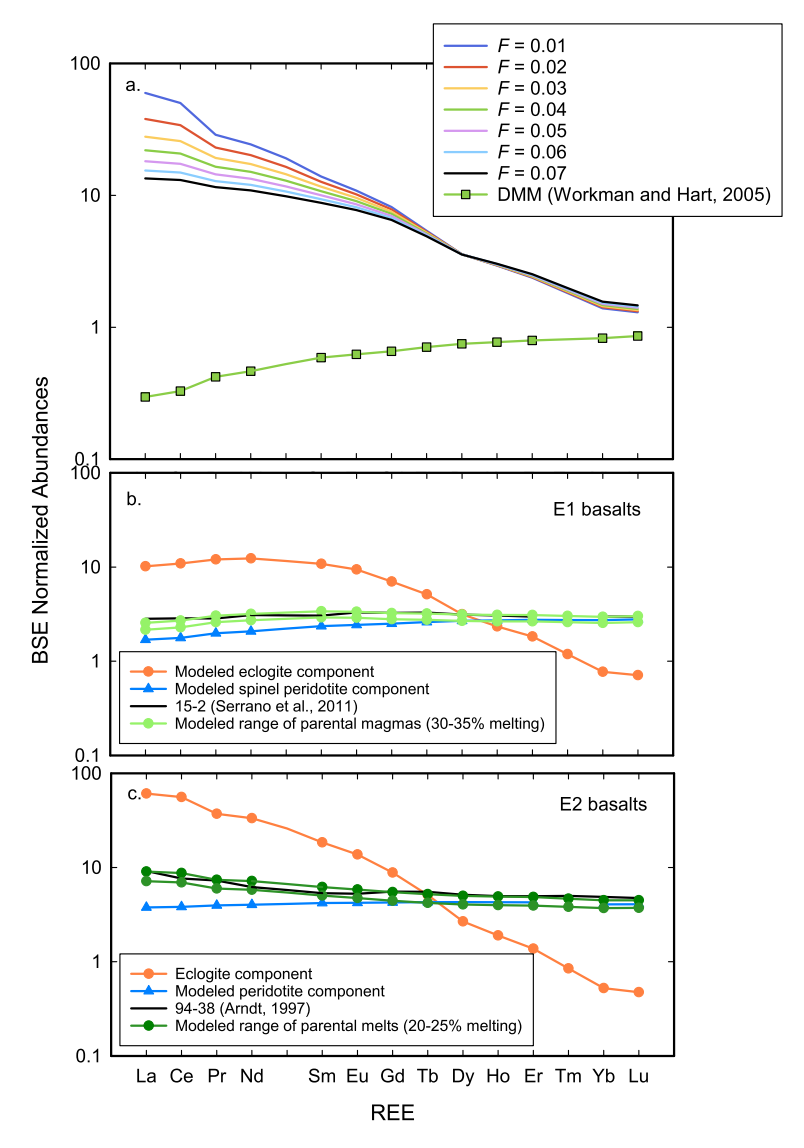


Fig. 7. Various modeled melts in comparison to the least concentrated (least differentiated) E1 and E2-basalts sampled from Gorgona Island as an upper bound for the primary magmas for each group. Pyroxenite and peridotite melt components are calculated separately before being mixed together in the manner of Sobolev et al. (2007).

e-basalts discussed in this study owing to the enrichment caused in MREE relative to sample trace element compositions. As pyroxenite likely started melting at greater depth, the pyroxenite component of the melt is considered at a higher degree of melting than that of peridotite for both cases. This degree of pyroxenite inferred to have contributed to the e-basalts is consistent with recent estimates of the degree of pyroxenite present in the Galapagos plume (Soderman et al., 2023). In the case of E1 basalts, the pyroxenite component is inferred to have melted to high degrees (up to F = 0.35) compared to the peridotite component, calculated to F = 0.25-0.30. The high degree of melting calculated for the peridotite component to generate the low concentrations specific to E1 basalts suggests that either melting started in the garnet peridotite regime, or that the source was significantly more depleted in composition than used in calculations. As aggregated fractional melts are almost indistinguishable from batch melting calculations for REEs (e.g., Johnson et al., 1990; Révillon et al., 2000b), the calculations performed here are considered to applicable to pooled melts. The high degree of melting inferred for the e-basalts suggest the melts have pooled as they rose to the surface. The hybrid peridotite sources of the E1 and E2 basalts are inferred to be slightly more depleted in LREE than the Caribbean Oceanic Plateau mantle plume source modeled in Hastie et al. (2016).

5.5. Pyroxenite as a recycled component and the survival of primordial heterogeneity through a separate peridotite mantle source

The ¹⁴²Nd/¹⁴⁴Nd isotope ratios of the komatiites measured in this study are similar to the average modern-day mantle, indicating either: i) that source differentiation took place after \sim 4.0 Ga or ii) that any isotope anomalies resulting from silicate mantle differentiation occurring at >4.0 Ga were re-homogenized prior to the melting of the source that produced the Gorgona lavas. The high ³He/⁴He ratios of the G1 and G2 komatiites and picrite of this study on the other hand, which are sourced from the hottest parts of the Galapagos plume (Arndt et al., 1997; Kerr et al., 1996; Kerr, 2005), characterize a depleted source with high ³He/⁴He ratios. Serrano et al. (2011) suggested that the lavas from the Caribbean Large Igneous Province, including those from Gorgona Island, may have been generated solely from a slab window setting without the involvement of a plume. However, the high ${}^{3}\text{He}/{}^{4}\text{He}$ ratios ranging up to 45 RA for the Gorgona lavas observed in this study, far exceed the canonical MORB average (8 \pm 1 $R_{\text{A}};$ Graham, 2002) and unequivocally indicate influences from a plume source, as also proposed earlier by Hastie and Kerr (2010).

The magnitude of ³He/⁴He ratios overall are observed to correlate with the inferred degree of pyroxenite present in the dif-

ferent lava types. Picrites, which are inferred to have originated from a depleted peridotite mantle source (Arndt et al., 1997; Kerr, 2005; Révillon et al., 2000a), exhibit the most depleted trace element concentrations among the different Gorgona rock types while also having the highest ³He/⁴He values within the Caribbean Large Igneous Province. The e-basalt, which is deduced to have a significant pyroxenite component in its source, exhibit a low RA of 6.9, whereas the d-basalt exhibits an RA that is slightly higher, at 10.7 R_A . Therefore, the pyroxenite component of the different sources is inferred to have overprinted the primordial ³He/⁴He signatures of the depleted mantle component and is thus deduced to be recycled. In addition, it is inferred that the low concentrations of trace elements in lavas derived from a more depleted peridotite source, such as those of the Gorgona komatiites and picrites, enable the preservation of their high ³He/⁴He ratios. Similarly, global correlations in high ${}^{3}\text{He}/{}^{4}\text{He}$ ratios and depleted $\varepsilon^{143}\text{Nd}$ signatures (e.g., Starkey et al., 2009) suggest that depleted sources are intrinsic to the preservation of primitive ${}^{3}\mathrm{He}/{}^{4}\mathrm{He}$ ratios. The depleted $\varepsilon^{143}\mathrm{Nd}$ signatures of the high ³He/⁴He mantle reservoir however, indicates that such a reservoir has undergone partial melting and although not entirely outgassed, is no longer strictly primordial.

While it has been proposed that 182 W/ 184 W isotope anomalies are exclusively preserved in mantle domains with the least amount of recycled material (Jackson et al., 2020), our analysis of the Gorgona e-basalts suggests that there are exceptions. Interestingly, the e-basalts from Gorgona have been reported to have $\mu^{182} W$ isotope anomalies averaging -10 ppm, whereas the W isotopes of some Gorgona komatiites are unresolved from the average mantle (Walker et al., 2021). Combined with the ³He/⁴He data, this may suggest an anticorrelation between the ¹⁸²W/¹⁸⁴W isotope ratios and ³He/⁴He data for at least a subset of Gorgona lavas, contrary to established trends for OIBs worldwide and lavas throughout the Caribbean Large Igneous Province (Mundl-Petermeier et al., 2020, 2019; Mundl et al., 2017). As an abundance of pyroxenite is deduced in the sources of the e-basalts compared to other Gorgona lavas, which is suggested to have affected their ³He/⁴He ratios, a mechanism is needed to explain the presence of ¹⁸²W/¹⁸⁴W isotope anomalies.

Model calculations involving the simultaneous involvement of pyroxenite and two kinds of peridotite sources in the melting of the e-basalts attest to the persistence of $\mu^{182}W$ anomalies compared to $\mu^{142} \mathrm{Nd}$ isotope variability. As kimberlites (formerly, Group I kimberlites) have been observed to evolve from a reservoir exhibiting BSE-like ε^{176} Hf and ε^{143} Nd isotopes for the past 2.5 Gyr (Woodhead et al., 2019) while simultaneously exhibiting W isotope anomalies (Nakanishi et al., 2021), calculations are carried out by characterizing the BSE peridotite reservoir used in this study with a $\mu^{182}W$ anomaly of -25 ppm, inferred from W isotope measurements of modern lavas from the Galapagos plume (Mundl-Petermeier et al., 2020). Using the degree of pyroxenite calculated for the sources of the two groups of e-basalts, the $\mu^{182}W$ signatures of the e-basalts are simultaneously modeled with ε^{143} Nd in Fig. 8. Despite the involvement of recycled pyroxenite in source of the e-basalts and a separate peridotite source lacking $\mu^{182} W$ anomalies, $\mu^{182} W$ anomalies are demonstrated to persist. On the other hand, the lack of $\mu^{182}W$ anomalies in some komatiites, which are thought to be derived from the hottest and deepest parts of the Galapagos plume, may signify the lack of $\mu^{182}W$ anomalies of the mantle source with connections to the core-mantle boundary, particularly where the Galapagos plume has been suggested to be rooted (Cottaar et al., 2022; Trela et al., 2017). This in turn would argue against a unique core-origin mechanism as the hypothesis to explain high ³He/⁴He ratios and modern-day $\mu^{182}W$ anomalies. The lack of $\mu^{142}Nd$ anomalies for the depleted mantle source at the Galapagos plume additionally

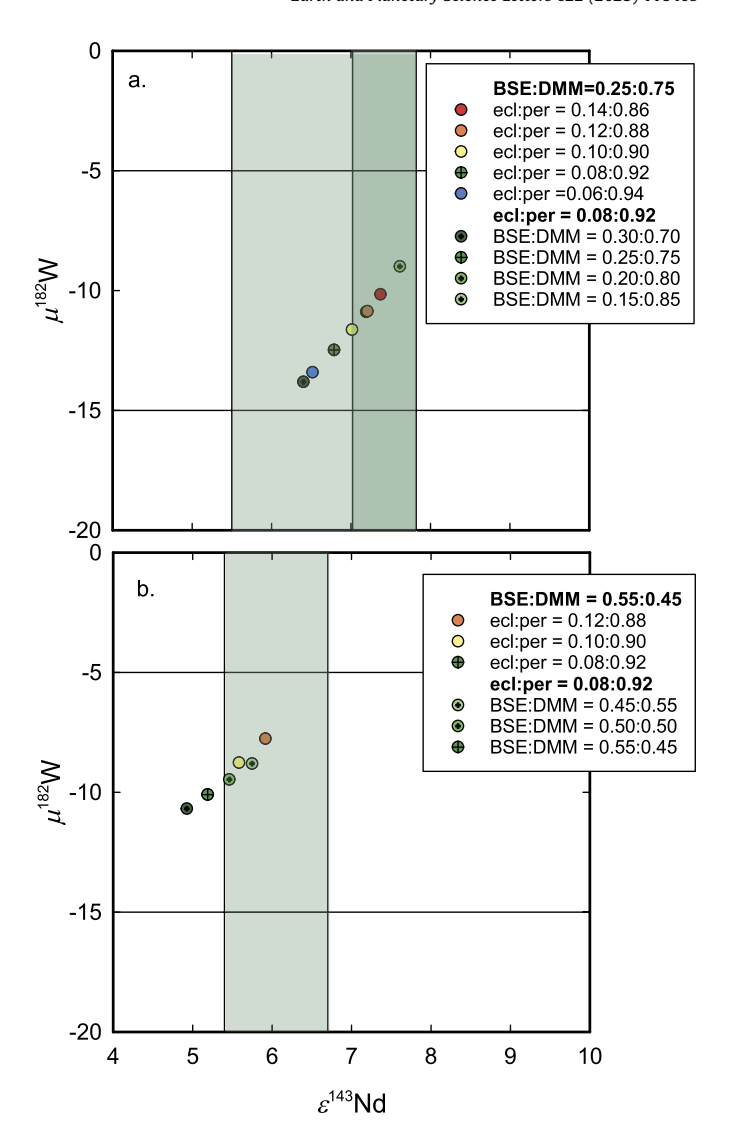


Fig. 8. Changes in the μ^{182} W and ε^{143} Nd values with respect to varying degrees of pyroxenite (labeled "ecl") and BSE vs DMM-type peridotite ("per") mantle reservoir involvement for (a) E1 basalts and (b) E2 basalts plotted alongside calculated REE patterns (Supplementary Material Fig. S1). The shaded areas bracket the range of ε^{143} Nd values observed for each type of e-basalt. The majority of observed ε^{143} Nd values for E1 basalts is between 7–8, with one sample at 5.6. The BSE peridotite component used in calculations is set to have a μ^{182} W of -25 after the data of Mundl-Petermeier et al. (2020) and is defined to have an ε^{143} Nd of 0.

suggests the absence of a reservoir anomalous in $\mu^{142} \rm Nd$ in this plume source stored at the core-mantle boundary.

These calculations may be applied to $\mu^{142}Nd$ isotopes to assess their preservation under analogous conditions. Much of the terrestrial μ^{142} Nd isotope variability is observed in the Archean and is limited in range, varying by ± 20 ppm and to a large extent, homogeneous by the Proterozoic (e.g., Hyung and Jacobsen, 2020). In comparison, the greatest degree of ¹⁴²Nd isotope anomalies in the modern-day mantle, which are relatively rare in comparison, are around ± 7 –8 ppm (2 $\sigma = \pm 4.4$ ppm; Peters et al., 2018). A BSE mantle source modified to exhibit a μ^{142} Nd value of -8, when mixed with the pyroxenite component, generate values of -2.1 and -2.8 ppm respectively for the E1 and E2 basalts, which are difficult to resolve with the typical precision of ¹⁴²Nd/¹⁴⁴Nd isotope measurements ($2\sigma = \pm 2$ –5 ppm) in comparison to 182 W/ 184 W isotope ratios. The μ^{142} Nd anomalies appear to be reduced to one third to a quarter of their original magnitude through this mixing process, in contrast with just half the original magnitude for analogous calculations involving $\mu^{182}W$ isotopes. The relative con-

centrations of the Nd and W present in the two different types of peridotite reservoirs and pyroxenite, governed by their partitioning behavior, are therefore key to preserving $\mu^{182}W$ anomalies. This difference in sensitivity to pyroxenite, may, in part, explain the longevity of $\mu^{182}W$ isotope anomalies originating from early silicate Earth differentiation relative to $\mu^{142} \mathrm{Nd}$ anomalies. Furthermore, these effects may be exacerbated by the initial magnitudes of $\mu^{142} Nd$ and $\mu^{182} W$ anomalies that may have developed during early silicate Earth differentiation. Fractionation of Sm and Nd owing to early silicate Earth differentiation has been suggested to be limited (Jacobsen and Harper, 1996), translating to the range of $\mu^{142} \text{Nd}$ variability ($\pm 20 \text{ ppm}$) observed in Archean terrains. In contrast, it is possible to envision an early Earth where $\mu^{182}W$ anomalies may have been more extreme in magnitude (≥22 ppm) owing to a greater degree of Hf/W fractionation during a process such as magma ocean crystallization.

With respect to He, the RA value of 45.1 observed for the rough mineral separates of the picrite sample in this study is among the highest ³He/⁴He ratios observed among mantle-derived rocks, close to what is observed at Baffin Island (~50 RA; e.g., Starkey et al., 2009; Willhite et al., 2019). The source of the Gorgona komatiites and picrites are also suggested to share similarities to those of the Baffin Island picrites, as noted by their highly depleted $\varepsilon^{143} \mathrm{Nd}$ signatures and lack of $^{142} \mathrm{Nd}/^{144} \mathrm{Nd}$ (de Leeuw et al., 2017) and 182 W/ 184 W isotope anomalies (Jansen et al., 2022). This may suggest the presence of a depleted mantle reservoir common to various mantle plumes that is high in ³He/⁴He ratios but not anomalous in ¹⁸²W/¹⁸⁴W nor ¹⁴²Nd/¹⁴⁴Nd isotopes, suggesting that tungsten isotope anomalies may not be fundamentally intrinsic to the high ³He/⁴He mantle reservoir. The shallow and steep trends among negative tungsten isotope anomalies and high ³He/⁴He ratios observed at various hot spots may thus reflect different proportions of reservoir involvement.

In general, ¹⁸²W/¹⁸⁴W anomalies are deemed to be more common across various OIBs (Mundl-Petermeier et al., 2020, 2019; Mundl et al., 2017; Peters et al., 2021; Rizo et al., 2019), in contrast to the rarity of ¹⁴²Nd/¹⁴⁴Nd isotope anomalies in modern-day samples (Andreasen et al., 2008; Cipriani et al., 2011; de Leeuw et al., 2017; Hyung and Jacobsen, 2020; Jackson and Carlson, 2012; Murphy et al., 2010; Peters et al., 2021, 2018). Tusch et al. (2022) proposed mafic Hadean restites as a possible reservoir for anomalous $\mu^{182}W$ isotope signatures. According to this idea, if the source of the $\mu^{182}W$ anomalies observed in the Gorgona e-basalts can be attributed to recycled Hadean restites from an upwelling mantle plume, they may be ascribed to the pyroxenite component of the source. The inferred peridotite source of the picrites, which are attributed to the deepest parts of the Galapagos plume (Arndt et al., 1997: Kerr. 2005: Révillon et al., 2000a), and various subductionzone systems proposed in context to the Caribbean Large Igneous Province (e.g., Duncan and Hargraves, 1984; Kerr et al., 1996; Pindell et al., 2006), suggest that the recycled pyroxenite source component of the e-basalts may be a more recent feature related to the tectonics of the region. Nonetheless, various considerations from model calculations, possible source contributions, and observations from the data suggest that $\mu^{182}W$ isotope anomalies may be most likely to survive mixing with recycled components among the three tracers $(^{3}\text{He})^{4}\text{He}$, $^{142}\text{Nd}/^{144}\text{Nd}$, and $^{182}\text{W}/^{184}\text{W})$ of primordial mantle heterogeneity. The presence or absence of ¹⁴²Nd/¹⁴⁴Nd, ¹⁸²W/¹⁸⁴W anomalies, and high ³He/⁴He signatures in modern-day terrestrial samples therefore likely reflect their varying degrees of sensitivity to the different overprinting mantle processes that have taken place since primordial Hadean silicate differentiation.

6. Summary and conclusion

The range of rock types at Gorgona Island reflect their diverse sources, with a significant source contribution of pyroxenite deduced for the e-basalts, and d-basalts to a lesser degree. Similar to previous inferences, komatiites and picrites are deduced to be derived from a peridotite source. E-basalts can be divided into two groups ("E1" and "E2") based on their trace element abundances. Using constraints from REE patterns, $\varepsilon^{143}\mathrm{Nd}$ isotopes, and the degree of pyroxenite involvement in the source based on major element analysis, the REE patterns of the e-basalts may be modeled as produced via melting of a 8% pyroxenite and a 92% peridotite source. The peridotite source may be modeled to be composed of two end-member components, a DMM-type depleted mantle source, and a BSE-type source.

New ³He/⁴He measurements of a range of Gorgona lavas exhibit high values up to 45.1 RA and strongly indicate a connection to a plume source that may be similar to that of the Baffin Island picrites. The ¹⁴²Nd/¹⁴⁴Nd isotope ratios of Gorgona komatiites in contrast, are indistinguishable from the modern-day bulk silicate Earth. The depleted mantle component of the Galapagos plume is characterized to be primitive in ³He/⁴He ratios but lacking 142Nd/144Nd isotope anomalies. Meanwhile, the low ³He/⁴He ratio of the e-basalt compared to other Gorgona lavas is attributed to the recycled pyroxenite component in the source. Calculations demonstrate the survival of ¹⁸²W/¹⁸⁴W isotope anomalies despite the presence of recycled pyroxenite, in contrast to ¹⁴²Nd/¹⁴⁴Nd isotope ratios, suggesting homogenization occurring on different timescales under similar conditions. Tungsten isotope anomalies are therefore inferred to be the most persistent among the three different tracers of the primordial mantle (182W/184W, ³He/⁴He, and ¹⁴²Nd/¹⁴⁴Nd) when met with the involvement of recycled pyroxenite in the source. The high ³He/⁴He ratios measured for the Gorgona lavas, which exhibit an unusual correlation with ¹⁸²W/¹⁸⁴W isotope variability, combined with the lack of 142Nd/144Nd isotope anomalies observed for the Gorgona komatiites, likely reflect the different degrees of sensitivity of the three isotope tracers to different terrestrial processes that developed, preserved, and/or differentially homogenized these signatures throughout time.

CRediT authorship contribution statement

Eugenia Hyung: Writing – review & editing, Writing – original draft, Visualization, Validation, Methodology, Investigation, Funding acquisition, Formal analysis, Data curation, Conceptualization. **Mauricio Ibañez-Mejia:** Writing – review & editing, Resources. **Yamirka Rojas-Agramonte:** Writing – review & editing, Resources.

Declaration of competing interest

The authors declare that they have no known competing financial interests or personal relationships that could have appeared to influence the work reported in this paper.

Data availability

Data will be made available on request.

Acknowledgements

We thank the editor, Rosemary Hickey-Vargas for handling the manuscript, and two anonymous reviewers for their constructive reviews. We additionally thank all those who have generously lent their resources and time to make this study happen: the Colombian National Park Services for granting the permit to visit the island and take samples, to Nils Suhr, Sarah Bonilla, and Ivan Bonilla

for their help collecting and transporting the samples, and to all the staff of the island for their support and hospitality during our visit. We thank Francois Tissot (FT) for providing the clean lab and instrumental facilities to process samples and measure trace elements and Nd isotopes at Caltech, Gerrit Budde for assisting in processing samples and generating the trace element data, Ken Farley and Jonathan Treffkorn for generating and providing the He data from their laboratory, Claire Bucholtz for providing lab facilities to measure loss on ignition, and George Rossman for providing access to his XRF instrument to measure major element compositions. In addition, we also thank Ming Zhen Yu for discussions on trace element modeling and Stein B. Jacobsen for helpful discussions and suggestions with respect to the manuscript. This project was funded by Caltech start-up funds to FT, and partially supported by the NSF postdoctoral fellowship award 2053045 to EH.

Appendix A. Supplementary material

Supplementary material related to this article can be found online at https://doi.org/10.1016/j.epsl.2023.118409.

References

- Aitken, B.G., Echeverría, L.M., 1984. Petrology and geochemistry of komatiites and tholeiites from Gorgona Island, Colombia. Contrib. Mineral. Petrol. 86, 94–105. https://doi.org/10.1007/BF00373714.
- Al-Hakkani, M.F., 2019. Guideline of inductively coupled plasma mass spectrometry "ICP-MS": fundamentals, practices, determination of the limits, quality control, and method validation parameters. SN Appl. Sci. 1, 1–15. https://doi.org/10.1007/s42452-019-0825-5.
- Andreasen, R., Sharma, M., Subbarao, K.V., Viladkar, S.G., 2008. Where on Earth is the enriched Hadean reservoir? Earth Planet. Sci. Lett. 266, 14–28. https://doi. org/10.1016/j.epsl.2007.10.009.
- Arndt, N.T., Kerr, A.C., Tarney, J., 1997. Dynamic melting in plume heads: the formation of Gorgona komatiites and basalts. Earth Planet. Sci. Lett. 146, 289–301. https://doi.org/10.1016/S0012-821X(96)00219-1.
- Baker, M.B., Stolper, E.M., 1994. Determining the composition of high-pressure mantle melts using diamond aggregates. Geochim. Cosmochim. Acta 58, 2811–2827. https://doi.org/10.1016/0016-7037(94)90116-3.
- Balbas, A.M., Farley, K.A., 2020. Constraining in situ cosmogenic nuclide paleoproduction rates using sequential lava flows during a paleomagnetic field strength low. Chem. Geol. 532, 119355. https://doi.org/10.1016/j.chemgeo.2019. 119355.
- Boschman, L.M., van Hinsbergen, D.J.J., Torsvik, T.H., Spakman, W., Pindell, J.L., 2014. Kinematic reconstruction of the Caribbean region since the Early Jurassic. Earth-Sci. Rev. 138, 102–136. https://doi.org/10.1016/j.earscirev.2014.08.007.
- Brügmann, G.E., Arndt, N.T., Hofmann, A.W., Tobschall, H.J., 1987. Noble metal abundances in komatiite suites from Alexo, Ontario and Gorgona Island, Colombia. Geochim. Cosmochim. Acta 51, 2159–2169. https://doi.org/10.1016/0016-7037(87)90265-1
- Cipriani, A., Bonatti, E., Carlson, R.W., 2011. Nonchondritic ¹⁴²Nd in suboceanic mantle peridotites. Geochem. Geophys. Geosyst. 12, 1–8. https://doi.org/10.1029/2010GC003415.
- Cottaar, S., Martin, C., Li, Z., Parai, R., 2022. The root to the Galápagos mantle plume on the core-mantle boundary. Seismica 1 (1), 1–12. https://doi.org/10.26443/seismica.v1i1.197.
- de Leeuw, G.A.M., Ellam, R.M., Stuart, F.M., Carlson, R.W., 2017. ¹⁴²Nd/¹⁴⁴Nd inferences on the nature and origin of the source of high ³He/⁴He magmas. Earth Planet. Sci. Lett. 472, 62–68. https://doi.org/10.1016/j.epsl.2017.05.005.
- Dietrich, V.J., Gansser, A., Sommerauer, J., Cameron, W.E., 1981. Palaeogene komatiites from Gorgona Island, East Pacific—A primary magma for ocean floor basalts? Geochem. J. 15, 141–162. https://doi.org/10.2343/geochemj.15.141.
- Duncan, R.A., Hargraves, R.B., 1984. Plate tectonic evolution of the Caribbean region in the mantle reference frame. In: Bonini, W.E., Hargraves, R.B., Shagam, R. (Eds.), The Caribbean-South America Plate Boundary and Regional Tectonics. Geological Society of America Memoir, pp. 81–93.
- Dupré, B., Echeverría, L.M., 1984. Pb isotopes of Gorgona Island (Colombia): isotopic variations correlated with magma type. Earth Planet. Sci. Lett. 67, 186–190. https://doi.org/10.1016/0012-821X(84)90113-4.
- Echeverría, L.M., 1980. Tertiary or Mesozoic komatiites from Gorgona Island, Colombia: field relation and geochemistry. Contrib. Mineral. Petrol. 73, 253–266. https://doi.org/10.1007/BF00381444.
- Echeverría, L.M., Aitken, B.G., 1986. Pyroclastic rocks: another manifestation of ultramafic volcanism on Gorgona Island, Colombia. Contrib. Mineral. Petrol. 92, 428–436. https://doi.org/10.1007/BF00374425.

- Ferrick, A.L., Korenaga, J., 2023. Long-term core-mantle interaction explains W-He isotope heterogeneities. Proc. Natl. Acad. Sci. USA 120, 1–8. https://doi.org/10. 1073/pnas.2215903120.
- French, S.W., Romanowicz, B., 2015. Broad plumes rooted at the base of the Earth's mantle beneath major hotspots. Nature 525, 95–99. https://doi.org/10.1038/nature14876
- Graham, D.W., 2002. Noble gas isotope geochemistry of mid-ocean ridge and ocean island basalts: characterization of mantle source reservoirs. Rev. Mineral. Geochem. 47, 247–317. https://doi.org/10.2138/rmg.2002.47.8.
- Hastie, A.R., Fitton, J.G., Kerr, A.C., McDonald, I., Schwindrofska, A., Hoernle, K., 2016. The composition of mantle plumes and the deep Earth. Earth Planet. Sci. Lett. 444, 13–25. https://doi.org/10.1016/j.epsl.2016.03.023.
- Hastie, A.R., Kerr, A.C., 2010. Mantle plume or slab window?: physical and geochemical constraints on the origin of the Caribbean oceanic plateau. Earth-Sci. Rev. 98, 283–293. https://doi.org/10.1016/j.earscirev.2009.11.001.
 Hyung, E., Jacobsen, S.B., 2020. The ¹⁴²Nd/¹⁴⁴Nd variations in mantle-derived rocks
- Hyung, E., Jacobsen, S.B., 2020. The ¹⁴²Nd/¹⁴⁴Nd variations in mantle-derived rocks provide constraints on the stirring rate of the mantle from the Hadean to the present. Proc. Natl. Acad. Sci. USA 117, 14738–14744. https://doi.org/10.1073/pnas.2006950117.
- Hyung, E., Sedaghatpour, F., Larsen, T., Neumann, E.-R., Eriksen, Z.T., Petaev, M.I., Jacobsen, S.B., 2023. A peridotite source for strongly alkalic ultrabasic HIMU lavas of the Oslo Rift, Norway. Chem. Geol. 622, 121377. https://doi.org/10.1016/ j.chemgeo.2023.121377.
- Hyung, E., Tissot, F.L.H., 2021. Routine high-precision Nd isotope analyses: an optimized chromatographic purification scheme. J. Anal. At. Spectrom. 36, 1946–1959. https://doi.org/10.1039/d1ja00169h.
- Jackson, M.G., Blichert-Toft, J., Halldórsson, S.A., Mundl-Petermeier, A., Bizimis, M., Kurz, M.D., Price, A.A., Harðardóttir, S., Willhite, L.N., Breddam, K., Becker, T.W., Fischer, R.A., 2020. Ancient helium and tungsten isotopic signatures preserved in mantle domains least modified by crustal recycling. Proc. Natl. Acad. Sci. USA 117, 30993–31001. https://doi.org/10.1073/pnas.2009663117.
- Jackson, M.G., Carlson, R.W., 2012. Homogeneous superchondritic ¹⁴²Nd/¹⁴⁴Nd in the mid-ocean ridge basalt and ocean island basalt mantle. Geochem. Geophys. Geosyst. 13, 1–10. https://doi.org/10.1029/2012GC004114.
- Jacobsen, S.B., Harper, C.L., 1996. Earth Processes: Reading the Isotopic Code. In: Basu, A., Hart, S. (Eds.), Geophysical Mongraph 95, pp. 47–74.
- Jansen, M.W., Tusch, J., Münker, C., Bragagni, A., Avanzinelli, R., Mastroianni, F., Stuart, F.M., Kurzweil, F., 2022. Upper mantle control on the W isotope record of shallow level plume and intraplate volcanic settings. Earth Planet. Sci. Lett. 585, 117507. https://doi.org/10.1016/j.epsl.2022.117507.
- Jochum, K.P., Nohl, U., Herwig, K., Lammel, E., Stoll, B., Hofmann, A.W., 2005. GeoReM: a new geochemical database for reference materials and isotopic standards. Geostand. Geoanal. Res. 29, 333–338. https://doi.org/10.1111/j.1751-908X 2005 tb00904 x
- Johnson, K.T.M., Dick, H.J.B., Shimizu, N., 1990. Melting in the oceanic upper mantle: an ion microprobe study of diopsides in abyssal peridotites. J. Geophys. Res. 95, 2661–2678. https://doi.org/10.1029/JB095iB03p02661.
- Kerr, A.C., 2005. La Isla de Gorgona, Colombia: a petrological enigma? Lithos 84, 77–101. https://doi.org/10.1016/j.lithos.2005.02.006.
- Kerr, A.C., Arndt, N.T., 2001. A note on the IUGS reclassification of the high-Mg and picritic volcanic rocks. J. Petrol. 42, 2169–2171. https://doi.org/10.1093/ petrology/42.11.2169.
- Kerr, A.C., Marriner, G.F., Arndt, N.T., Tarney, J., Nivia, A., Saunders, A.D., Duncan, R.A., 1996. The petrogenesis of Gorgona komatiites, picrites and basalts: new field, petrographic and geochemical constraints. Lithos 37, 245–260. https://doi.org/10.1016/0024-4937(95)00039-9.
- Kerr, A.C., Tarney, J., 2005. Tectonic evolution of the Caribbean and northwestern South America: the case for accretion of two Late Cretaceous oceanic plateaus. Geology 33, 269–272. https://doi.org/10.1130/G21109.1.
- Kinzler, R.J., Grove, T.L., 1992. Primary magmas of mid-ocean ridge basalts 1. Experiments and methods. J. Geophys. Res. 97, 6885–6906. https://doi.org/10.1029/911B02840.
- Kleine, T., Münker, C., Mezger, K., Palme, H., 2002. Rapid accretion and early core formation on asteroids and the terrestrial planets from Hf-W chronometry. Nature 418, 952–955. https://doi.org/10.1038/nature00982.
- Kogiso, T., Hirose, K., Takahashi, E., 1998. Melting experiments on homogeneous mixtures of peridotite and basalt: application to the genesis of ocean island basalts. Earth Planet. Sci. Lett. 162, 45–61. https://doi.org/10.1016/S0012-821X(98)00156-3.
- Kruijer, T.S., Touboul, M., Fischer-Godde, M., Bermingham, K.R., Walker, R.J., Kleine, T., 2014. Protracted core formation and rapid accretion of protoplanets. Science 344, 1150–1154. https://doi.org/10.1126/science.1251766.
- Le Bas, M.J., 2000. IUGS reclassification of the high-Mg and picritic volcanic rocks. J. Petrol. 41, 1467–1470. https://doi.org/10.1093/petrology/41.10.1467.
- Mallik, A., Dasgupta, R., 2012. Reaction between MORB-eclogite derived melts and fertile peridotite and generation of ocean island basalts. Earth Planet. Sci. Lett. 329–330, 97–108. https://doi.org/10.1016/j.epsl.2012.02.007.
- Marks, N.E., Borg, L.E., Hutcheon, I.D., Jacobsen, B., Clayton, R.N., 2014. Samarium-neodymium chronology and rubidium-strontium systematics of an Allende calcium-aluminum-rich inclusion with implications for ¹⁴⁶Sm half-life. Earth Planet. Sci. Lett. 405, 15–24. https://doi.org/10.1016/j.epsl.2014.08.017.

- McDonough, W.F., Sun, S.-s., 1995. The composition of the Earth. Chem. Geol. 120, 223–253. https://doi.org/10.1016/0009-2541(94)00140-4.
- Meissner, F., Schmidt-Ott, W.D., Ziegeler, L., 1987. Half-life and α-ray energy of 146 Sm. Z. Phys. 327, 171–174. https://doi.org/10.1007/BF01292406.
- Mundl-Petermeier, A., Walker, R.J., Fischer, R.A., Lekic, V., Jackson, M.G., Kurz, M.D., 2020. Anomalous ¹⁸²W in high ³He/⁴He ocean island basalts: fingerprints of Earth's core? Geochim. Cosmochim. Acta 271, 194–211. https://doi.org/10.1016/j.gca.2019.12.020.
- Mundl-Petermeier, A., Walker, R.J., Jackson, M.G., Blichert-toft, J., Kurz, M.D., Halldórsson, S.A., 2019. Temporal evolution of primordial tungsten-182 and ³He/⁴He signatures in the Iceland mantle plume. Chem. Geol. 525, 245–259. https://doi.org/10.1016/j.chemgeo.2019.07.026.
- Mundl, A., Touboul, M., Jackson, M.G., Day, J.M.D., Kurz, M.D., Lekic, V., Helz, R.T., Walker, R.J., 2017. Tungsten-182 heterogeneity in modern ocean island basalts. Science 356, 66–69. https://doi.org/10.1126/science.aal4179.
- Murphy, D.T., Brandon, A.D., Debaille, V., Burgess, R., Ballentine, C., 2010. In search of a hidden long-term isolated sub-chondritic ¹⁴²Nd/¹⁴⁴Nd reservoir in the deep mantle: implications for the Nd isotope systematics of the Earth. Geochim. Cosmochim. Acta 74, 738–750. https://doi.org/10.1016/j.gca.2009.10.005.
- Nakanishi, N., Giuliani, A., Carlson, R.W., Horan, M.F., Woodhead, J., Pearson, D.G., Walker, R.J., 2021. Tungsten-182 evidence for an ancient kimberlite source. Proc. Natl. Acad. Sci. USA 118, 1–8. https://doi.org/10.1073/pnas.2020680118.
- Pertermann, M., Hirschmann, M.M., 2003. Partial melting experiments on a MORB-like pyroxenite between 2 and 3 GPa: constraints on the presence of pyroxenite in basalt source regions from solidus location and melting rate. J. Geophys. Res. 108, 1–17. https://doi.org/10.1029/2000|B000118.
- Peters, B.J., Carlson, R.W., Day, J.M.D., Horan, M.F., 2018. Hadean silicate differentiation preserved by anomalous ¹⁴²Nd/¹⁴⁴Nd ratios in the Réunion hotspot source. Nature 555, 89–93. https://doi.org/10.1038/nature25754.
- Peters, B.J., Mundl-Petermeier, A., Carlson, R.W., Walker, R.J., Day, J.M.D., 2021. Combined lithophile-siderophile isotopic constraints on Hadean processes preserved in ocean island basalt sources. Geochem. Geophys. Geosyst. 22, 1–20. https://doi.org/10.1029/2020GC009479.
- Pindell, J., Kennan, L., Stanek, K.P., Maresch, W.V., Draper, G., 2006. Foundations of Gulf of Mexico and Caribbean evolution: eight controversies resolved. Geol. Acta 4, 303–341.
- Révillon, S., Arndt, N.T., Chauvel, C., Hallot, E., 2000a. Geochemical study of ultramafic volcanic and plutonic rocks from Gorgona Island, Colombia: the plumbing system of an oceanic plateau. J. Petrol. 41, 1127–1153. https://doi.org/10.1093/ petrology/41.7.1127.
- Révillon, S., Hallot, E., Arndt, N.T., Chauvel, C., Duncan, R.A., 2000b. A complex history for the Caribbean plateau: petrology, geochemistry, and geochronology of the Beata Ridge, South Hispaniola. J. Geol. 108, 641–661. https://doi.org/10.1086/317953.
- Révillon, S., Chauvel, C., Arndt, N.T., Pik, R., Martineau, F., Fourcade, S., Marty, B., 2002. Heterogeneity of the Caribbean plateau mantle source: Sr, O and He isotopic compositions of olivine and clinopyroxene from Gorgona Island. Earth Planet. Sci. Lett. 205, 91–106. https://doi.org/10.1016/S0012-821X(02)01003-
- Rizo, H., Andrault, D., Bennett, N.R., Humayun, M., Brandon, A., Vlastelic, I., Moine, B., Poirier, A., Bouhifd, M.A., Murphy, D.T., 2019. ¹⁸²W evidence for core-mantle interaction in the source of mantle plumes. Geochem. Perspect. Lett. II, 6–11. https://doi.org/10.7185/geochemlet.1917.
- Serrano, L., Ferrari, L., Martinez, M.L., Petrone, C.M., Jaramillo, C., 2011. An integrative geologic, geochronologic and geochemical study of Gorgona Island, Colombia: implications for the formation of the Caribbean Large Igneous Province. Earth Planet. Sci. Lett. 309, 324–336. https://doi.org/10.1016/j.epsl.2011.07.011.

- Shorttle, O., Maclennan, J., 2011. Compositional trends of Icelandic basalts: implications for short-length scale lithological heterogeneity in mantle plumes. Geochem. Geophys. Geosyst. 12, Q110008. https://doi.org/10.1029/2011GC003748.
- Sobolev, A.V., Hofmann, A.W., Kuzmin, D.V., Yaxley, G.M., Arndt, N.T., Chung, S.-L., Danyushevsky, L.V., Elliott, T., Frey, F.A., Garcia, M.O., Gurenko, A.A., Kamenetsky, V.S., Kerr, A.C., Krivolutskaya, N.A., Matvienkov, V.V., Nikogosian, I.K., Rocholl, A., Sigurdsson, I.A., Sushchevskaya, N.M., Teklay, M., 2007. The amount of recycled crust in sources of mantle-derived melts. Science 316, 412–417. https://doi.org/10.1126/science.1138113.
- Soderman, C.R., Shorttle, O., Gazel, E., Geist, D.J., Matthews, S., Williams, H.M., 2023. The evolution of the Galápagos mantle plume. Sci. Adv. 9, 1–9. https://doi.org/ 10.1126/sciadv.add5030.
- Starkey, N.A., Stuart, F.M., Ellam, R.M., Fitton, J.G., Basu, S., Larsen, L.M., 2009. Helium isotopes in early Iceland plume picrites: constraints on the composition of high ³He/⁴He mantle. Earth Planet. Sci. Lett. 277, 91–100. https://doi.org/10.1016/j.epsl.2008.10.007.
- Storey, M., Mahoney, J.J., Kroenke, L.W., Saunders, A.D., 1991. Are oceanic plateaus sites of komatiite formation? Geology 19, 376–379. https://doi.org/10.1130/0091-7613(1991)019<0376:AOPSOK>2.3.CO;2.
- Trela, J., Gazel, E., Sobolev, A.V., Moore, L., Bizimis, M., Jicha, B., Batanova, V.G., 2017.
 The hottest lavas of the Phanerozoic and the survival of deep Archaean reservoirs. Nat. Geosci. 10, 451–456. https://doi.org/10.1038/ngeo2954.
- Trela, J., Vidito, C., Gazel, E., Herzberg, C., Class, C., Whalen, W., Jicha, B., Bizimis, M., Alvarado, G.E., 2015. Recycled crust in the Galápagos plume source at 70 Ma: implications for plume evolution. Earth Planet. Sci. Lett. 425, 268–277. https://doi.org/10.1016/j.epsl.2015.05.036.
- Tusch, J., Hoffmann, J.E., Hasenstab, E., Fischer-Gödde, M., Marien, C.S., Wilson, A.H., Münker, C., 2022. Long-term preservation of Hadean protocrust in Earth's mantle. Proc. Natl. Acad. Sci. USA 119, 1–12. https://doi.org/10.1073/pnas. 2120241119
- Vockenhuber, C., Bichler, M., Golser, R., Kutschera, W., Priller, A., Steier, P., Winkler, S., 2004. ¹⁸²Hf, a new isotope for AMS. Nucl. Instrum. Methods Phys. Res., Sect. B 223–224, 823–828. https://doi.org/10.1016/j.nimb.2004.04.152.
- Walker, R.J., Mundl-Petermeier, A., Puchtel, I., Echeverría, L.M., Ludwig, K., Nicklas, R., Estaban, G., Devitre, C., 2021. New insights to the origin of ultramafic-mafic magmatism, Gorgona Island, Colombia. In: AGU Fall Meeting Abstracts. DI24A-06.
- Walker, R.J., Storey, M., Kerr, A.C., Tarney, J., Arndt, N.T., 1999. Implications of ¹⁸⁷Os isotopic heterogeneities in a mantle plume: evidence from Gorgona Island and Curação. Geochim. Cosmochim. Acta 63, 713–728. https://doi.org/10.1016/s0016-7037(99)00041-1.
- Walter, M.J., 1998. Melting of garnet peridotite and the origin of komatiite and depleted lithosphere. J. Petrol. 39, 29–60. https://doi.org/10.1093/petroj/39.1.29.
- Willhite, L.N., Jackson, M.G., Blichert-Toft, J., Bindeman, I., Kurz, M.D., Halldórsson, S.A., Harðardóttir, S., Gazel, E., Price, A.A., Byerly, B.L., 2019. Hot and heterogenous high-³He/⁴He components: new constraints from Proto-Iceland plume lavas From Baffin Island. Geochem. Geophys. Geosyst. 20, 5939–5967. https://doi.org/10.1029/2019GC008654.
- Woodhead, J., Hergt, J., Giuliani, A., Maas, R., Phillips, D., Pearson, D.G., Nowell, G., 2019. Kimberlites reveal 2.5-billion-year evolution of a deep, isolated mantle reservoir. Nature 573, 578–581. https://doi.org/10.1038/s41586-019-1574-8.
- Workman, R.K., Hart, S.R., 2005. Major and trace element composition of the depleted MORB mantle (DMM). Earth Planet. Sci. Lett. 231, 53–72. https://doi.org/10.1016/j.epsl.2004.12.005.
- Yang, Z.F., Zhou, J.H., 2013. Can we identify source lithology of basalt? Sci. Rep. 3, 1–7. https://doi.org/10.1038/srep01856.